

Title	Carrier recombination lifetime in InAs thin films bonded on low-k flexible substrates
Author(s)	Suzuki, Toshi-kazu; Hayato Takita; Cong Thanh Nguyen; Iiyama, Koichi
Citation	AIP Advances, 2(4): 042105-1-042105-6
Issue Date	2012-10-02
Type	Journal Article
Text version	publisher
URL	http://hdl.handle.net/10119/12907
Rights	© Copyright 2012 Author(s). This article is distributed under a Creative Commons Attribution 3.0 Unported License. The following article appeared in Toshi-kazu Suzuki, Hayato Takita, Cong Thanh Nguyen and Koichi Iiyama, AIP Advances, 2(4), 042105 (2012) and may be found at http://dx.doi.org/10.1063/1.4757943
Description	



Carrier recombination lifetime in InAs thin films bonded on low- k flexible substrates

Toshi-kazu Suzuki,^{1,a} Hayato Takita,¹ Cong Thanh Nguyen,¹
and Koichi Iiyama²

¹Center for Nano Materials and Technology, Japan Advanced Institute of Science and Technology (JAIST), 1-1 Asahidai, Nomi, Ishikawa 923-1292, Japan

²School of Electrical and Computer Engineering, Kanazawa University, Kakuma, Kanazawa, Ishikawa 920-1192, Japan

(Received 22 August 2012; accepted 21 September 2012; published online 2 October 2012)

We investigated carrier recombination in InAs thin films obtained by epitaxial lift-off and van der Waals bonding on low- k flexible substrates. Photoconductors are fabricated from the InAs thin films bonded on flexible substrates, and also from films grown on GaAs(001) substrates. By irradiation of 1.55- μm -wavelength laser light with intensity modulation, we characterized frequency responses of the InAs photoconductors by S -parameter measurements. From an analysis of the frequency dependence of the S -parameters, we obtained carrier recombination lifetimes, which are long for the InAs thin films bonded on flexible substrates in comparison with those grown on GaAs(001), attributed to the lower dislocation density in the former. Copyright 2012 Author(s). This article is distributed under a Creative Commons Attribution 3.0 Unported License. [<http://dx.doi.org/10.1063/1.4757943>]

I. INTRODUCTION

Heterogeneous integration of narrow-gap III-V compound semiconductors on foreign host substrates can lead to superior or novel functionalities, such as optical and ultra-high-frequency signal processing. As a method of the heterogeneous integration, we investigated epitaxial lift-off (ELO) and van der Waals bonding (VWB) of the narrow-gap compound semiconductors obtained by lattice-mismatched growth with nano-scale thin sacrificial layers,^{1,2} while most studies on ELO-VWB had been restricted to GaAs lattice-matched systems^{3,4} with a few exceptions.⁵ Among the narrow-gap compound semiconductors, InAs is important for ultra-high-speed electron devices,⁶⁻¹³ mid-infrared optical devices,^{6,14} and also interband tunnel devices.¹⁵⁻¹⁷ In the previous work, we demonstrated ELO-VWB processes to realize formation of high-quality InAs thin films bonded on low dielectric constant (low- k) flexible substrates ($k \lesssim 3$), exhibiting very high electron mobilities.¹⁸ The low- k flexible substrates with extremely high resistivities, such as polyethylene terephthalate (PET) substrates, have advantages for high-speed applications due to low parasitic capacitance and low leakage current, and also for light-weight, portable, and flexible electronic apparatus applications. In addition, we recently elucidated electron scattering mechanisms dominating electron mobilities in the InAs thin films on low- k flexible substrates,¹⁹ giving insights for applications to unipolar devices, such as field-effect transistors. On the other hand, carrier recombination dynamics are important for applications to bipolar devices, such as optical devices, and are sensitive to crystal qualities. The purpose of this work is to investigate carrier recombination dynamics in the InAs thin films bonded on low- k flexible substrates, in comparison with films grown on GaAs(001) substrates. While there are recently several reports on carrier recombination lifetime measurements for InAs-related superlattices by time-resolved photoluminescence²⁰ and modulation response technique,^{21,22} in this work, we fabricated photoconductors from the InAs thin films bonded on flexible substrates, and

^aAuthor to whom correspondence should be addressed; electronic mail: tosikazu@jaist.ac.jp



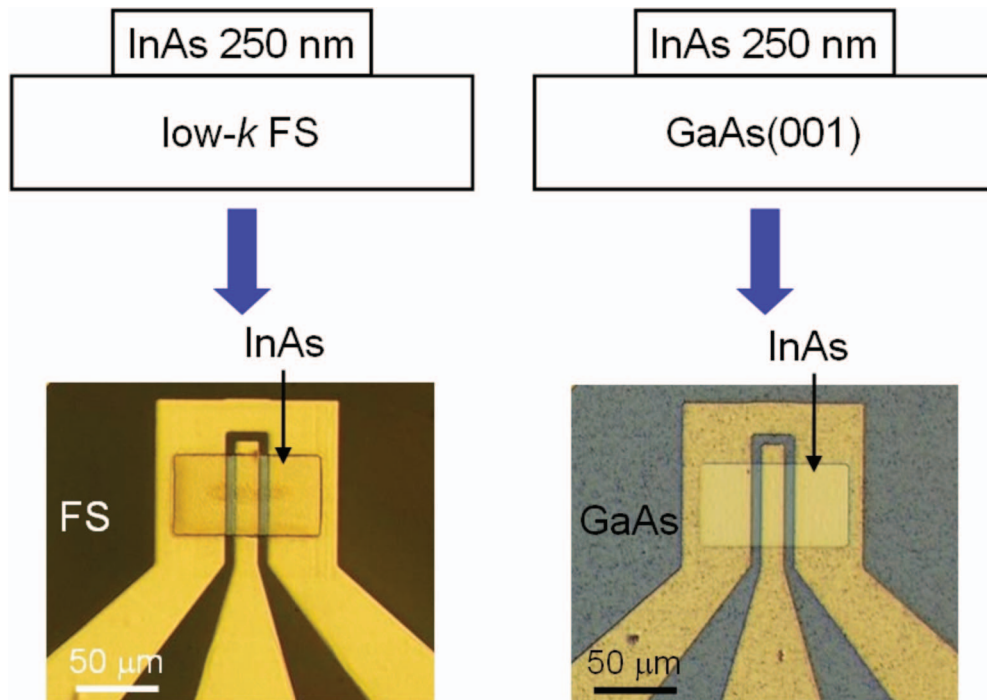


FIG. 1. Using InAs thin films of 250 nm thickness on a low- k flexible substrate (FS) and a GaAs(001) substrate, we fabricated InAs-on-FS (left) and InAs-on-GaAs (right) photoconductors, whose channel length and width of 6 μm and 100 μm , respectively.

also from the films grown on GaAs(001) substrates, for characterization of carrier recombination dynamics. Because of the InAs bandgap of 0.36 eV, photocarriers are excited by irradiation of 1.55- μm -wavelength laser light with intensity modulation. The frequency responses of the InAs photoconductors are characterized by S -parameter measurements, whose analysis gives carrier recombination lifetimes. This is the first report on carrier recombination dynamics in the InAs films obtained by ELO-VWB.

II. FABRICATION OF PHOTOCONDUCTORS

By means of molecular beam epitaxy, we grew a heterostructure for ELO-VWB, InAs layer (500 nm)/AlAs sacrificial layer (4 nm)/InAs buffer layer (2500 nm)/semi-insulating GaAs(001). The top InAs layer was separated and bonded on a host low- k flexible substrate (FS), PET coated by bisazide-rubber, by ELO using HF selective wet-etching of the sacrificial layer and normal VWB process as in the previous work.¹⁸ We also prepared InAs layer (500 nm)/semi-insulating GaAs(001), namely InAs directly grown on GaAs. After wet-etch thinning of the InAs layers down to 250 nm by H_3PO_4 -based etchant, we fabricated InAs-on-FS and InAs-on-GaAs photoconductors with InAs of 250 nm thickness, as shown in Fig. 1, where Ni/Au non-alloy Ohmic electrodes were formed. The channel length and width of 6 μm and 100 μm , respectively. As shown in the previous work, we obtain low dislocation densities and consequently high electron mobilities for the InAs-on-FS in comparison with the InAs-on-GaAs.¹⁸ In fact, we can estimate dislocation density in the InAs-on-FS, $\lesssim 1 \times 10^9 \text{ cm}^{-2}$ near the surface and $\sim 2 \times 10^9 \text{ cm}^{-2}$ at the interface, while the InAs-on-GaAs possesses estimated dislocation density $\sim 3 \times 10^9 \text{ cm}^{-2}$ near the surface and $> 10^{10} \text{ cm}^{-2}$ at the interface.²³ As a result, the InAs thin films of 250 nm thickness on FS and GaAs exhibit electron mobilities of 9600 $\text{cm}^2/\text{V}\cdot\text{s}$ and 5300 $\text{cm}^2/\text{V}\cdot\text{s}$, respectively, where the sheet electron concentration is $\sim 2 \times 10^{12} \text{ cm}^{-2}$ in spite of the undoped InAs films, owing to the Fermi level pinning above the conduction band bottom.^{24,25}

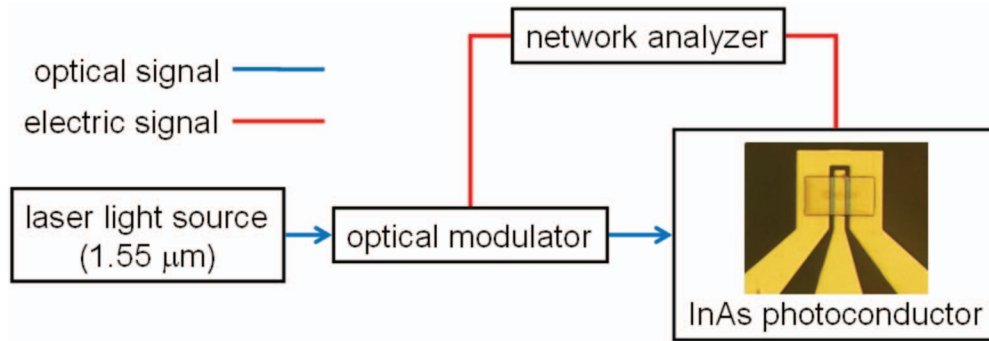


FIG. 2. The carrier recombination lifetime measurement setup. The 1.55- μm -wavelength laser light is modulated by an optical modulator and irradiated to the InAs photoconductors through an optical fiber. The optical modulator and the InAs photoconductor are connected to the 1st and 2nd ports of the network analyzer, respectively.

III. CHARACTERIZATION OF PHOTOCONDUCTORS

The fabricated InAs-on-FS and InAs-on-GaAs photoconductors were characterized, where we focused on room-temperature characterization because low temperature measurements unfortunately tend to cause damages of the InAs-on-FS photoconductors due to the thermal expansion coefficient difference between InAs and FS. We employed a carrier recombination lifetime measurement setup shown in Fig. 2, utilizing electron-hole generation in InAs by 1.55- μm -wavelength laser light excitation. The laser light is modulated by an optical modulator and irradiated to the InAs photoconductors through an optical fiber. The separation between the fiber head and the photoconductors is several hundred μm , and the light spot size is $\sim 50 \mu\text{m}$ with a power of 1.4 mW. The optical modulator, whose cut-off frequency is 11 GHz, makes $\sim 5\%$ power modulation of the light by -12 dBm RF signal from the 1st port of the network analyzer in the frequency range from 10 MHz to 10 GHz. As a result, the photoconductivity of the InAs photoconductors, connected to the 2nd port of the network analyzer and biased with 0.1–0.5 V, is modulated. We can characterize frequency responses of the InAs photoconductors by S -parameter measurements. In Fig. 3, we show the measured S -parameters for the InAs-on-FS photoconductors under several bias-voltages of 0.1–0.5 V. We can confirm unilateral properties by the extremely small S_{12} as a matter of course. From the S -parameters, we obtain a component of the non-dimensional Y parameter

$$y_{21} = \frac{-2S_{21}}{(1 + S_{11})(1 + S_{22}) - S_{12}S_{21}}, \quad (1)$$

which is directly related to the carrier recombination process as²⁶

$$|y_{21}|^2 \propto \frac{\tau_{\text{life}}^2}{\tau_{\text{tr}}^2} \frac{1}{1 + \omega^2 \tau_{\text{life}}^2}, \quad (2)$$

where τ_{life} is the carrier recombination lifetime and τ_{tr} is the channel transit time. Figure 4 shows frequency dependence of $|y_{21}|^2$ for several bias-voltages of 0.1–0.5 V. Since the results are consistent with Eq. (2), indicating effectiveness of this measurement method, we can obtain the carrier recombination lifetime τ_{life} . In Fig. 5, we show obtained carrier recombination lifetimes as functions of the bias-voltage. The lifetimes are in the sub-ns order, and long for the InAs-on-FS in comparison with the InAs-on-GaAs. Moreover, we observe the lifetime slightly depending on the bias-voltage for the InAs-on-FS, while the almost constant lifetime is obtained for the InAs-on-GaAs. Although the true mechanism is not elucidated, we assume that this is related to heat release properties. The InAs-on-FS, in comparison with the InAs-on-GaAs, has a poor heat release property and consequently prominent temperature increase by self-heating, which may influence the lifetime.

We also carried out Poisson-Schrödinger calculation²⁷ of electronic states in the InAs film as in.¹⁹ Figure 6 shows the bandbending and the electron distribution in the InAs film. The position along the thickness direction is denoted by z with the origin at the center of the thickness. The electron distribution is given by the electron density $\rho(z) = \sum_i \rho_i(z) = \sum_i n_i |\psi_i(z)|^2$, where $\rho_i(z)$ is

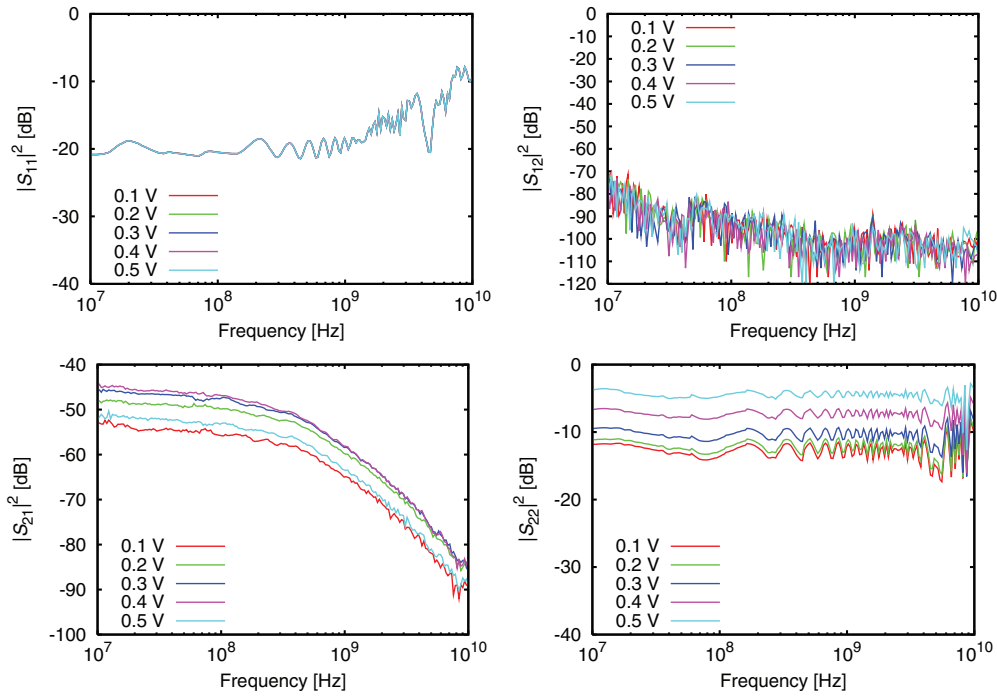


FIG. 3. Measured S -parameters for the InAs-on-FS photoconductors under several bias-voltages of 0.1–0.5 V.

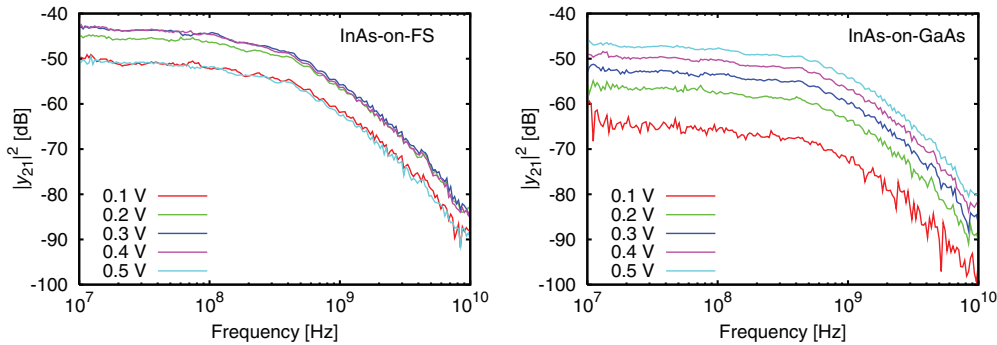


FIG. 4. Frequency dependence of $|y_{21}|^2$ obtained from measured S -parameters for the InAs-on-FS and InAs-on-GaAs photoconductors under several bias-voltages of 0.1–0.5 V.

the i -th subband electron density, obtained by the i -th subband sheet electron concentration n_i and the i -th subband eigen wavefunction $\psi_i(z)$. Owing to the Fermi level pinning above the conduction band bottom, the electron distribution exhibits accumulation near the top and bottom surfaces, given by two main independent conduction electron layers corresponding to $\rho_0(z)$ and $\rho_1(z)$, namely the electron density of the ground and the 1st excited subband, where the two subbands are degenerate. We find the peak electron density $\simeq 3.7 \times 10^{17} \text{ cm}^{-3}$ in the accumulation region near the top and bottom surfaces. Since the carrier recombination lifetime by CHCC Auger recombination is given by $\tau_A = 1/\gamma n^2$, where $\gamma \simeq 6.0 \times 10^{-27} \text{ cm}^6/\text{s}$ is the Auger coefficient of InAs²⁸ and n is the electron density, the peak electron density $\simeq 3.7 \times 10^{17} \text{ cm}^{-3}$ in the accumulation region near the top and bottom surfaces gives the Auger lifetime $\tau_A \simeq 1.2 \text{ ns}$. This is slightly larger than the obtained carrier recombination lifetime τ_{life} . This suggests that, although the lifetime is mainly dominated by the Auger recombination in the accumulation region near the top and bottom surfaces, there are additional recombination mechanisms which are strong (weak) for the InAs-on-GaAs (InAs-on-FS). We consider that the additional recombination mechanisms are related to dislocations, whose

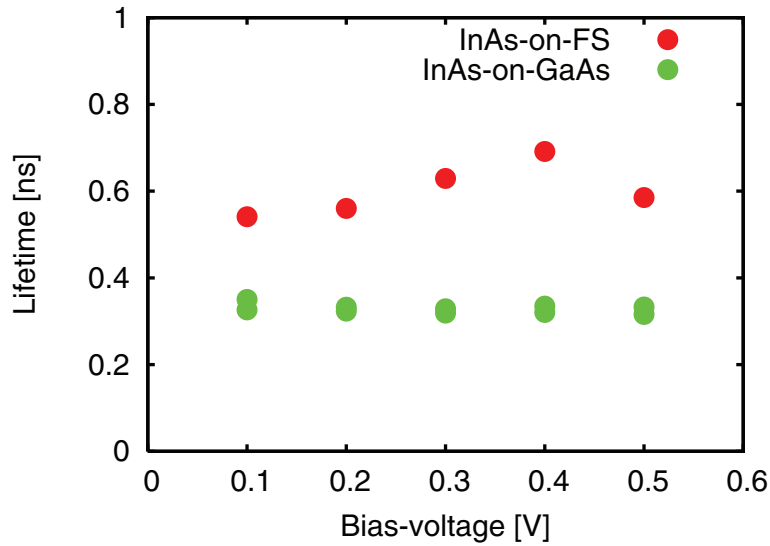


FIG. 5. Carrier recombination lifetimes as functions of the bias-voltage for the InAs-on-FS and InAs-on-GaAs.

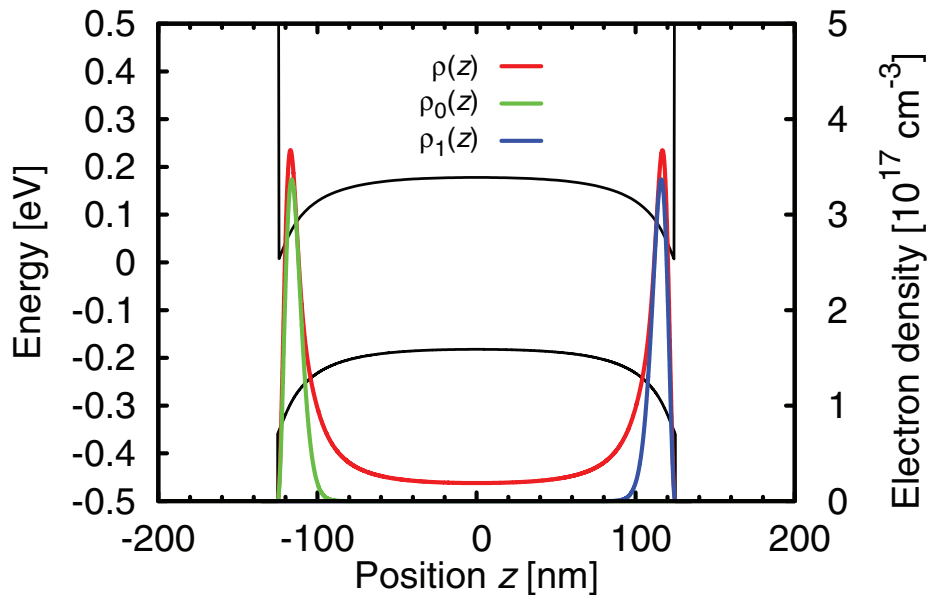


FIG. 6. Bandbending and electron distribution in the InAs film, obtained by Poisson-Schrödinger calculation.

density is high (low) for the InAs-on-GaAs (InAs-on-FS); the lifetime difference is attributed to the dislocation density difference, and is consistent with the mobility difference. It should be noted that the diffusion length $\sqrt{D\tau_{\text{life}}}$, where $D \sim 10 \text{ cm}^2/\text{s}$ is the hole diffusion constant, is larger than the InAs thickness 250 nm, which is consistent with the dominant recombination near the surface.

IV. SUMMARY

In summary, we investigated carrier recombination in InAs thin films obtained by epitaxial lift-off and van der Waals bonding on low- k FS. From the InAs thin films bonded on FS, and also from films grown on GaAs(001), we fabricated photoconductors for carrier recombination lifetime measurements. The frequency responses of the InAs photoconductors are characterized by S -parameter measurements, under irradiation of 1.55- μm -wavelength laser light with intensity

modulation. As a result, we obtained carrier recombination lifetimes of sub-ns order; they are longer for the InAs-on-FS than for the InAs-on-GaAs. Even though the carrier recombination is dominated by the Auger process, there are additional recombination mechanisms, whose difference is attributed to the dislocation density difference, consistent with the mobility difference.

ACKNOWLEDGMENTS

This work was partially supported by a research grant from the Foundation for Technology Promotion of Electronic Circuit Board.

- ¹ Y. Jeong, M. Shindo, M. Akabori, and T. Suzuki, *Appl. Phys. Express* **1**, 021201 (2008).
- ² Y. Jeong, M. Shindo, H. Takita, M. Akabori, and T. Suzuki, *Phys. Stat. Sol. C* **5**, 2787 (2008).
- ³ M. Konagai, M. Sugimoto, and K. Takahashi, *J. Cryst. Growth* **45**, 277 (1978).
- ⁴ E. Yablonovitch, T. Gmitter, J. P. Harbison, and R. Bhat, *Appl. Phys. Lett.* **51**, 2222 (1987).
- ⁵ J. Fastenau, E. Özbay, G. Tuttle, and F. Laabs, *J. Electron. Mater.* **24**, 757 (1995).
- ⁶ A. Milnes and A. Polyakov, *Mater. Sci. Eng. B* **18**, 237 (1993).
- ⁷ H. Kroemer, *Physica E* **20**, 196 (2004).
- ⁸ B. R. Bennett, R. Magno, J. B. Boos, W. Kruppa, and M. G. Ancona, *Solid-State Electron.* **49**, 1875 (2005).
- ⁹ D.-H. Kim and J. del Alamo, *IEEE Electron Device Lett.* **31**, 806 (2010).
- ¹⁰ N. Li, E. S. Harmon, J. Hyland, D. B. Salzman, T. P. Ma, Y. Xuan, and P. D. Ye, *Appl. Phys. Lett.* **92**, 143507 (2008).
- ¹¹ H. Ko, K. Takei, R. Kapadia, S. Chuang, H. Fang, P. W. Leu, K. Ganapathi, E. Plis, H. S. Kim, S.-Y. Chen, M. Madsen, A. C. Ford, Y.-L. Chueh, S. Krishna, S. Salahuddin, and A. Javey, *Nature* **468**, 286 (2010).
- ¹² K. Takei, S. Chuang, H. Fang, R. Kapadia, C.-H. Liu, J. Nah, H. S. Kim, E. Plis, S. Krishna, Y.-L. Chueh, and A. Javey, *Appl. Phys. Lett.* **99**, 103507 (2011).
- ¹³ K. Takei, H. Fang, S. B. Kumar, R. Kapadia, Q. Gao, M. Madsen, H. S. Kim, C.-H. Liu, Y.-L. Chueh, E. Plis, S. Krishna, H. A. Bechtel, J. Guo, and A. Javey, *Nano Lett.* **11**, 5008 (2011).
- ¹⁴ Z. Yin and X. Tang, *Solid-State Electron.* **51**, 6 (2007).
- ¹⁵ Q. Zhang, W. Zhao, and A. Seabaugh, *IEEE Electron Device Lett.* **27**, 297 (2006).
- ¹⁶ M. Luisier and G. Klimeck, *IEEE Electron Device Lett.* **30**, 602 (2009).
- ¹⁷ A. C. Ford, C. W. Yeung, S. Chuang, H. S. Kim, E. Plis, S. Krishna, C. Hu, and A. Javey, *Appl. Phys. Lett.* **98**, 113105 (2011).
- ¹⁸ H. Takita, N. Hashimoto, C. T. Nguyen, M. Kudo, M. Akabori, and T. Suzuki, *Appl. Phys. Lett.* **97**, 012102 (2010).
- ¹⁹ C. T. Nguyen, H.-A. Shih, M. Akabori, and T. Suzuki, *Appl. Phys. Lett.* **100**, 232103 (2012).
- ²⁰ D. Donetsky, S. P. Svensson, L. E. Vorobjev, and G. Belenky, *Appl. Phys. Lett.* **95**, 212104 (2009).
- ²¹ S. Svensson, D. Donetsky, D. Wang, H. Hier, F. Crowne, and G. Belenky, *J. Cryst. Growth* **334**, 103 (2011).
- ²² E. H. Steenbergen, B. C. Connelly, G. D. Metcalfe, H. Shen, M. Wraback, D. Lubyshev, Y. Qiu, J. M. Fastenau, A. W. K. Liu, S. Elhamri, O. O. Cellek, and Y.-H. Zhang, *Appl. Phys. Lett.* **99**, 251110 (2011).
- ²³ Y. Jeong, H. Choi, and T. Suzuki, *J. Cryst. Growth* **301–302**, 235 (2007).
- ²⁴ L. Ö. Olsson, C. B. M. Andersson, M. C. Håkansson, J. Kanski, L. Ilver, and U. O. Karlsson, *Phys. Rev. Lett.* **76**, 3626 (1996).
- ²⁵ H. Yamaguchi, R. Dreyfus, Y. Hirayama, and S. Miyashita, *Appl. Phys. Lett.* **78**, 2372 (2001).
- ²⁶ M. DiDomenico, Jr., and O. Svelto, *Proceedings of the IEEE* **52**, 136 (1964).
- ²⁷ G. L. Snider, Computer Program 1D Poisson/Schrödinger: A Band Diagram Calculator (<http://www.nd.edu/~gsnider>, University of Notre Dame, Notre Dame, Indiana).
- ²⁸ J. R. Lindle, J. R. Meyer, C. A. Hoffman, F. J. Bartoli, G. W. Turner, and H. K. Choi, *Appl. Phys. Lett.* **67**, 3153 (1995).